ELSEVIER

Coordination Chemistry Reviews
183 (1999) 117–138

COORDINATION CHEMISTRY REVIEWS

Inorganic crystal engineering using self-assembly of tailored building-blocks

Alexander J. Blake, Neil R. Champness, Peter Hubberstey, Wan-Sheung Li, Matthew A. Withersby, Martin Schröder *

School of Chemistry, The University of Nottingham, University Park, Nottingham NG7 2RD, UK

Received 17 November 1997

Contents

Abstract

The use of transition metal complexes of bridging bidentate ligands to construct predictable, multi-dimensional infinite networks is an area of chemistry which has received ever-increasing attention over recent years. This article will review the advances that have been made in this field of research and will illustrate how ligand design and the properties of the transition metal and counter-anion can be used to control network geometry and thus crystal structure. The range of network topologies and structural motifs that have been constructed thus far will be outlined with particular emphasis upon how specific arrays can be prepared via rational design of molecular building-blocks. The unusual phenomenon of interpenetration, or polycatenation, will be discussed and methods to achieve control over this effect will be highlighted.

* Corresponding author. Tel.: +44-115-9513490; Fax: +44-115-9513563; e-mail: m.schroder@nottingham.ac.uk

0010-8545/99/$ - see front matter
PII: S0010-8545(98)00173-8

Keywords: Inorganic crystal engineering; Inorganic supramolecular array; Network; Chain; Ladder; Sheet; Functionality

1. Introduction to inorganic supramolecular arrays

The construction of solid-state architectures and crystal engineering have become rapidly developing areas of research which have implications for the rational design of functional materials [1–4]. Much study has been centred upon the use of supramolecular contacts—in particular hydrogen bonding—between suitable molecules to generate multi-dimensional arrays or networks [1–3]. Although purely organic-based systems have become widely studied, their inorganic counterparts based upon coordination complexes have only recently received significant attention [4–13]. This work has been driven by the wide variety of network topologies that can be accessed by exploiting the variety of coordination geometries adopted by transition metals complexes. The structural motifs observed for these supramolecular arrays can to a certain extent be predicted and this has led to the development of a wide variety of architectures including adamantoid [4,6–9], cubic [10], ladder [11,12], honeycomb [13], helical staircase [14] and so-called brick-wall structures [15]. Although the overall structure is predominantly controlled by the coordination preferences of the transition metal and the ligand building blocks, more subtle effects such as anion control [14] and the use of the $\pi-\pi$ stacking [9] have been seen to have a profound effect upon network topology.

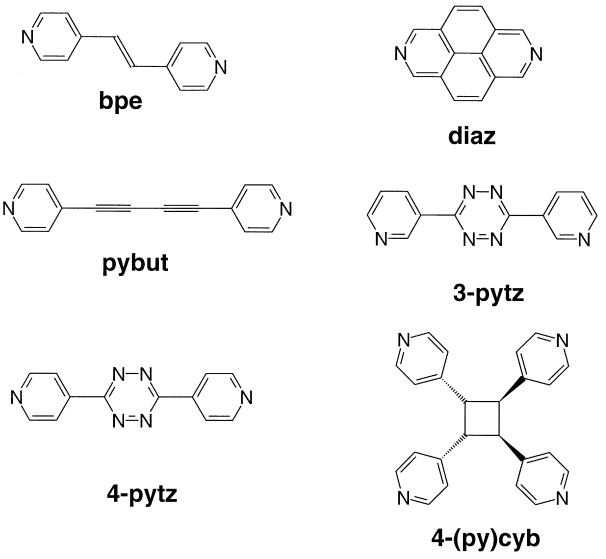

Scheme 1. Ligands investigated in the present study.

We have been investigating the effects of metal, ligand and anion functionality upon the structure of networks based upon adamantoid arrays and in Ag(I)–bipyridyl complexes that form chains, ladders and sheets. These areas will be discussed in turn, and some of the ligands used are shown in Scheme 1.

2. Adamantoid networks, control over interpenetration

The adamantoid structure, also known as a super-diamondoid structure, is a motif that can be observed for 3D structures based upon tetrahedral building blocks. The long-range structure consists of edge-sharing adamantoid units which build to form a 3D network (Fig. 1). Interpenetration (i.e. threading of one network through another) is observed in systems in which relatively large cavities are formed within the first polymeric array, and these need to be filled, in this case by other networks, so as to avoid collapse of the crystal lattice [4,16]. Adamantoid systems are particularly likely to exhibit interpenetration as the adamantoid units formed often have a large internal volume. Initial studies of organic adamantoid arrays were conducted by Ermer et al. on the structure of the 5-fold interpenetrating hydrogen-bonding lattice formed by adamantane-1,3,5,7-tetracarboxylic acid and its derivatives [16,17]. This research was subsequently extended to inorganic-based

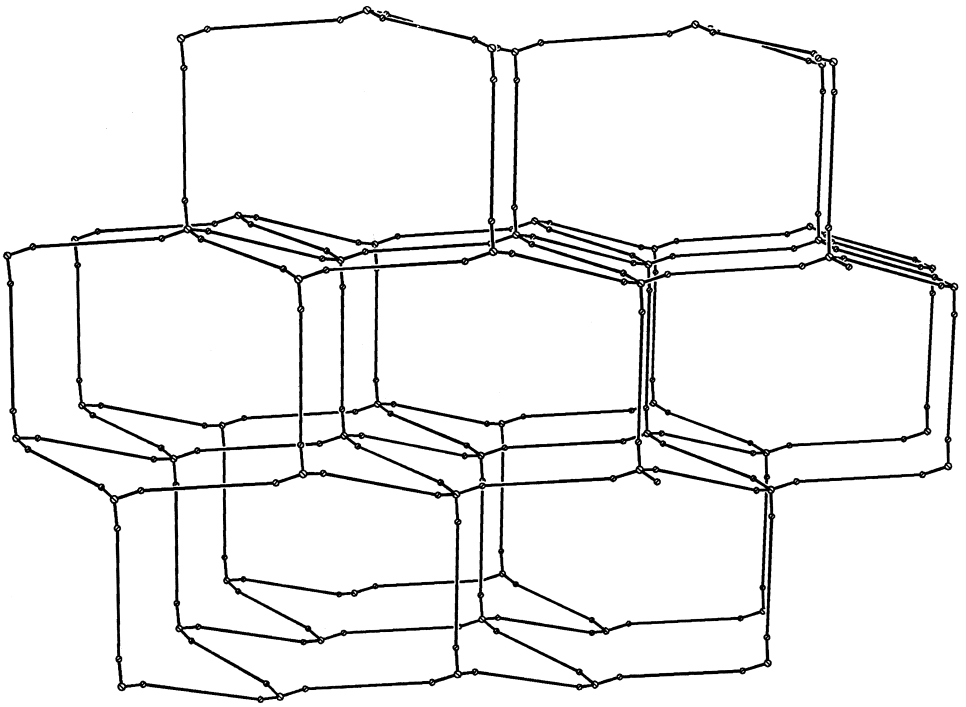

Fig. 1. Edge-sharing adamantoid units forming a three-dimensional network.

systems by Zaworotko et al. who used hydrogen-bonding interactions between $[M(CO)_3(\mu^3\text{-}OH)]_4$ (M = Mn, Re) and suitable hydrogen-bond acceptors to form a range of adamantoid arrays [18].

Examples of adamantoid arrays which do not rely upon hydrogen-bonding, but rather are based upon coordination complexes, are limited to Cu(I) and Ag(I) complexes of nitrogen ligands. These complexes can be divided into two types, those based upon 4,4′-bipyridyl and derivatives thereof [6–9], and those based upon dinitrile ligands such as 1,4-dicyanobenzene [4,19–22]. Our studies have focused primarily upon pyridyl-based ligands but, where appropriate, comparison and reference to nitrile-based systems will be made. In particular, our research has centred on the effect of ligand functionality upon the degree of interpenetration observed in adamantoid lattices based upon Cu(I)–bipyridyl complexes. Before our studies the only examples of adamantoid arrays based upon pyridyl ligands were $\{[Cu(4,4'\text{-bipy})_2]BF_4\}_\infty$ [6] and $\{[Ag(4,4'\text{-bipy})_2]CF_3SO_3\}_\infty$ [8]. In both cases 4-fold interpenetration was observed. We have prepared the complexes $\{[Cu(bpe)_2]BF_4\}_\infty$ [7] [bpe = *trans*-1,2-bis(4-pyridyl)ethene] and $\{[Cu(diaz)_2]PF_6\}_\infty$ [9] [diaz = 2,7-diazapyrene] in order to monitor the effects of variation of ligand length and of lateral bulk of the bipyridyl ligand upon the structure(s) observed.

The complex $\{[Cu(bpe)_2]BF_4\}_\infty$ was prepared by diffusing a solution of bpe in MeCN into a solution of $[Cu(MeCN)_4]PF_6$ in CH_2Cl_2 [7]. Crystals suitable for diffraction studies grew at the interface of the two solutions. The compound exists as a 3D adamantoid polymer in which each Cu(I) centre is coordinated in a tetrahedral geometry to four bpe ligands, Cu–N = 2.003(5)–2.084(6) Å, which are in turn coordinated to four other Cu(I) centres. The 3D structure builds through the formation of edge-sharing adamantoid units, (Fig. 1). The average Cu···Cu distance across the edge of each adamantoid unit is 13.55 Å creating large cavities within this first 3D lattice. These cavities are filled with four other $\{[Cu(bpe)_2]^+\}_\infty$ lattices so that a total of five independent adamantoid lattices, related by translational symmetry, interpenetrate throughout the 3D structure. The five independent lattices are polycatenated throughout the structure as illustrated in a simplified form by the five adamantoid units shown in Fig. 2. The channels running through the structure (Fig. 3) are parallel to the translation vector relating the five networks, and accommodate BF_4^- counter-ions and CH_2Cl_2 solvent molecules.

The coordination polymer $\{[Cu(diaz)_2]PF_6\}_\infty$ formed from the diffusion of $[Cu(MeCN)_4]PF_6$ in MeCN into a solution of 2,7-diazapyrene in PhCN also shows a 3D adamantoid network. The polymer was isolated as unusual triangular shaped crystals, and the single crystal X-ray structure determination confirms each Cu(I) centre to be tetrahedrally coordinated by four symmetry-equivalent diazapyrene ligands, Cu–N = 2.044(9) Å. The general coordination geometry resembles that of the corresponding bpe complex $\{[Cu(bpe)_2]BF_4\}_\infty$. However, in $\{[Cu(diaz)_2]PF_6\}_\infty$ spaces within each adamantoid array are filled by two other diamondoid networks and the three interpenetrating arrays are related to each other by a 90° rotation, (Fig. 4). This form of interpenetration contrasts with that observed for other Cu(I) and Ag(I) diamondoid networks which are related to each other by simple

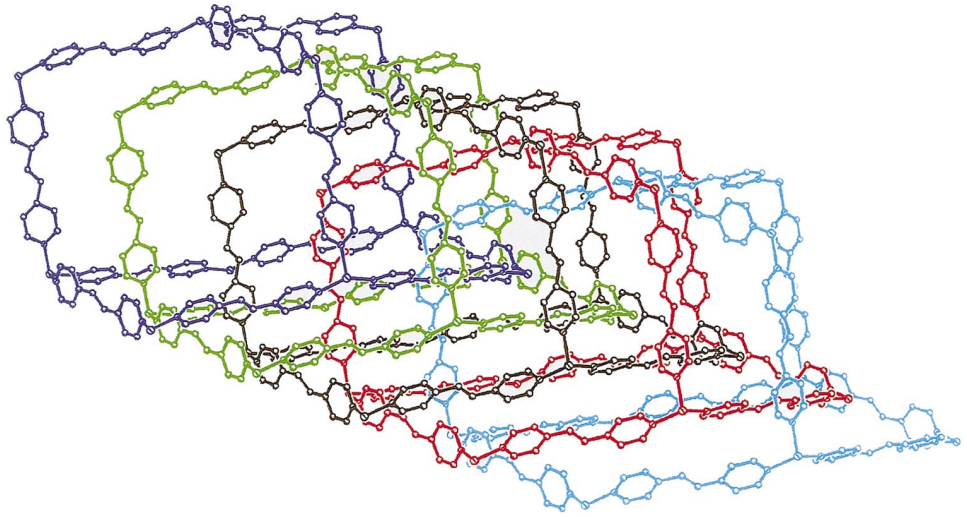

Fig. 2. The five independent interpenetrating adamantoid lattices of $\{[Cu(bpe)_2]^+\}_\infty$ (reproduced with permission from Ref. [7]).

translation. Adjacent lattices in $\{[Cu(diaz)_2]PF_6\}_\infty$ interact with each other via long-range face-to-face $\pi-\pi$ interactions of 3.469 Å between 2,7-diazapyrene liglands which are arranged so that the ligand N···N axes are mutually orthogonal.

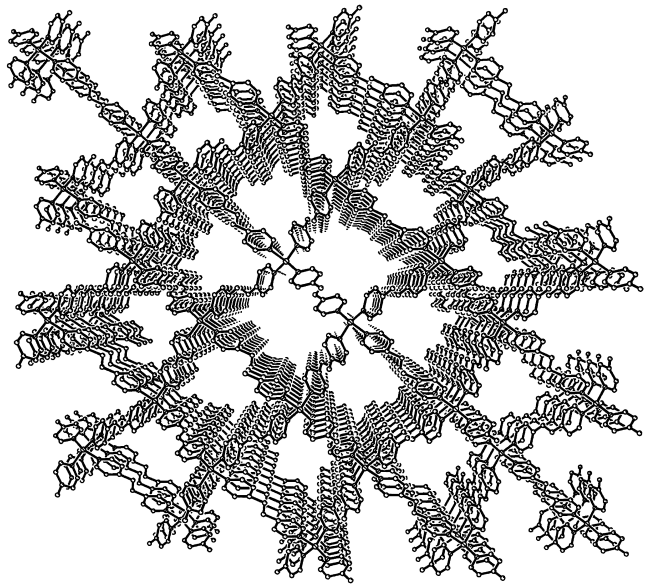

Fig. 3. View of the $\{[Cu(bpe)_2]^+\}_\infty$ network illustrating the channels that run through the structure accommodating BF_4^- counter-ions and CH_2Cl_2 solvent molecules.

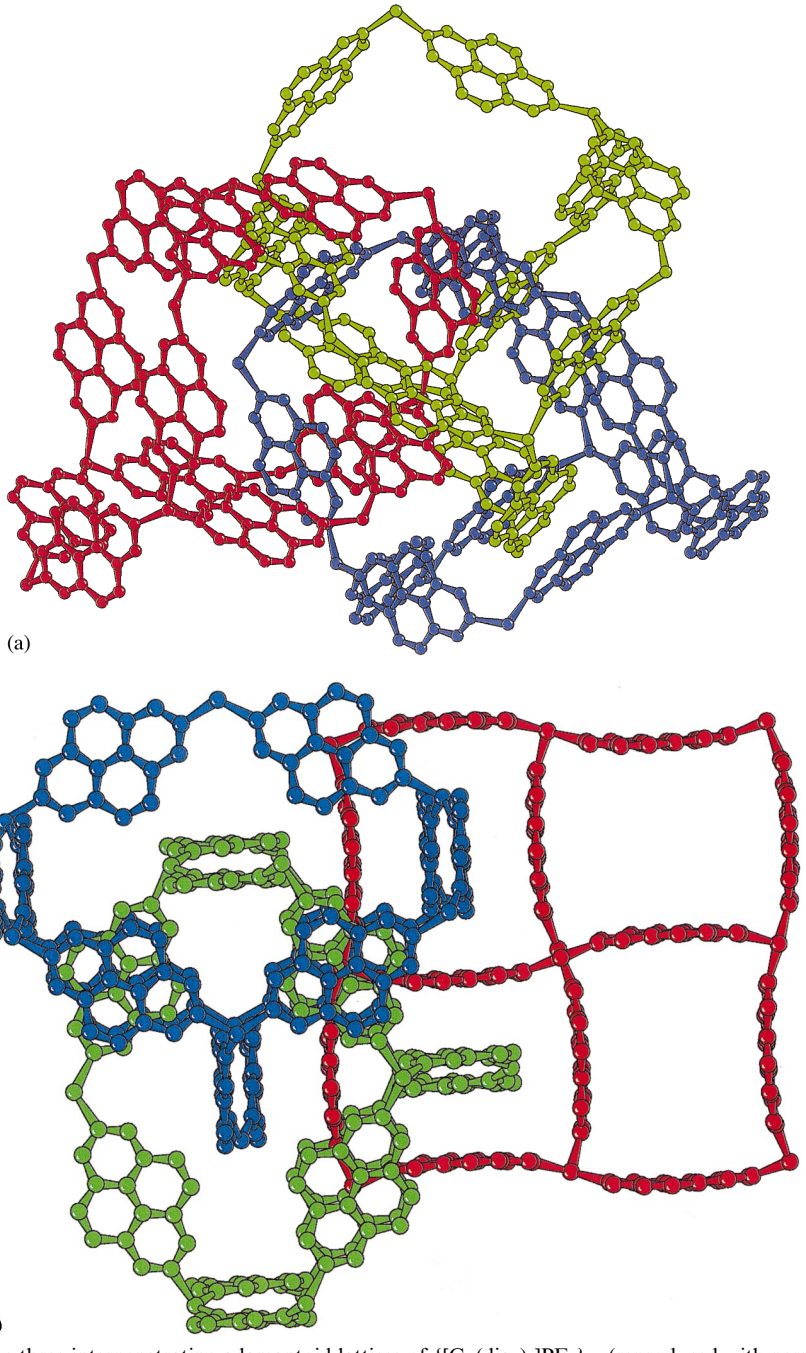

(a)

(b)

Fig. 4. The three interpenetrating adamantoid lattices of $\{[Cu(diaz)_2]PF_6\}_\infty$ (reproduced with permission from Ref. [9]).

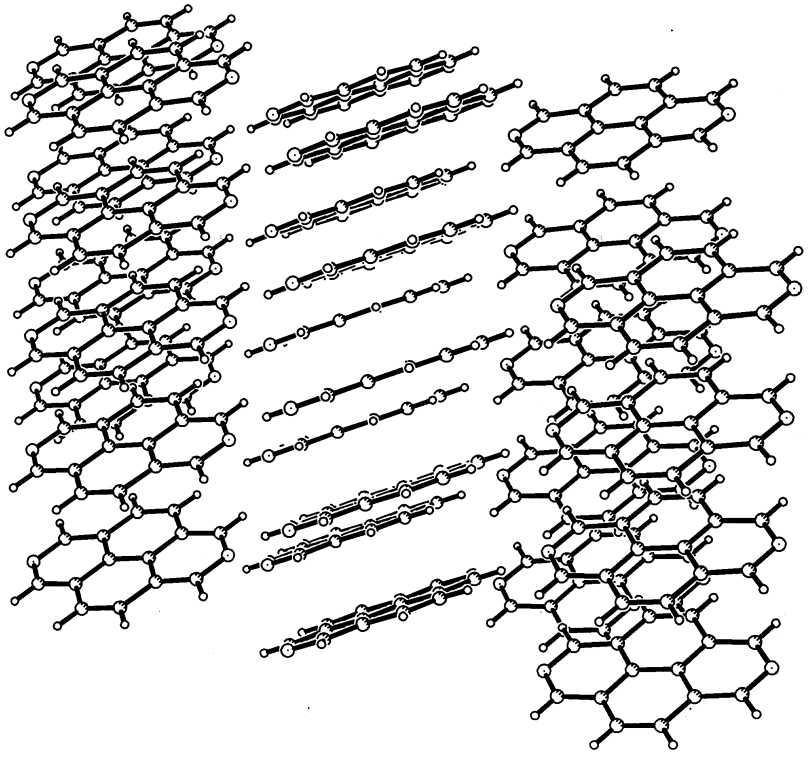

Fig. 5. View of the π–π stacking observed in the X-ray structure of 2,7-diazapyrene.

Interestingly, the X-ray structure of 2,7-diazapyrene as a metal-free ligand shows a separation of 3.450 Å between aromatic planes[1] (see Fig. 5) [23].

The structures of $\{[Cu(bpe)_2]BF_4\}_\infty$ and $\{[Cu(diaz)_2]PF_6\}_\infty$ are related to those observed for $\{[Cu(4,4'\text{-bipy})_2]BF_4\}_\infty$ [6] and $\{[Ag(4,4'\text{-bipy})_2]CF_3SO_3\}_\infty$ [8]. Four independent, interpenetrating lattices are observed in both the Cu(I) and Ag(I) adamantoid structures formed with 4,4′-bipy, in contrast to the five independent lattices observed for $\{[Cu(bpe)_2]BF_4\}_\infty$ [7] and the three observed for $\{[Cu(diaz)_2]PF_6\}_\infty$ [9]. Thus, lengthening the linking bipyridyl ligand by inserting a C=C double bond between the pyridyl units lengthens the edges of the adamantoid units to 13.55 Å (mean) in $\{[Cu(bpe)_2]BF_4\}_\infty$ [7] compared with 11.17 Å for $\{[Cu(4,4'\text{-bipy})_2]BF_4\}_\infty$ [6]. This increased length creates a larger cavity within the structure which is filled by the inclusion of an additional independent $\{[Cu(bpe)_2]^+\}_\infty$ lattice. Thus, by ligand design the degree of interpenetration has been increased from four independent lattices in $\{[Cu(4,4'\text{-bipy})_2]BF_4\}_\infty$ [6] to five in $\{[Cu(bpe)_2]BF_4\}_\infty$ [7], representing a degree of control over the degree of interpenetration observed.

[1] All π–π stacking distances are measured as the perpendicular distance between the planes of the ligands.

In the case of $\{[Cu(diaz)_2]PF_6\}_\infty$ [9] the ligand is slightly shorter than 4,4′-bipy, allowing a Cu···Cu distance of 10.90 Å along the edges of each adamantoid unit, compared to 11.17 Å in the case of $\{[Cu(4,4'\text{-bipy})_2]BF_4\}_\infty$ [6]. The observed decrease in the number of interpenetrating lattices (from four to three) might be accounted for by the shorter linking ligand, although this seems unlikely considering such a small decrease in Cu···Cu distance along the edge of the adamantoid unit. Increased $\pi-\pi$ interactions between adjacent lattices should encourage more efficient packing which would in turn encourage increasing numbers of independent lattices, in contrast to the decrease observed here. The most likely explanation for the decrease in the number of interpenetrating lattices appears to be the increase in the lateral bulk of the ligand which will reduce the volume of the voids within any given adamantoid lattice that has to be filled by other symmetry-related lattices. This represents identification of another possible factor controlling the degree and type of interpenetration in adamantoid lattices.

Adamantoid networks based on bifunctional linear ligands with nitrile ligating groups have also been studied for Cu(I) and Ag(I) complexes. In general a higher degree of interpenetration is observed for dinitrile adamantoid networks and this is attributed to the reduction in lateral steric bulk around each metal centre, which allows closer approach of adjacent adamantoid arrays. The main exception to this observation is the remarkable example of $\{[Cu(4,4',4'',4'''\text{-tetracyanotetraphenylmethane}]BF_4\cdot x C_6H_5NO_2\}_\infty$ reported by Robson et al. [19], which exists as a single adamantoid array with no interpenetration. Other examples of dinitrile-based adamantoid networks include $\{[Cu(1,4\text{-dicyanobenzene})_2]BF_4\}_\infty$ (five interpenetrating networks) [4], $\{[Ag(4,4'\text{-biphenyldicarbonitrile})_2]X\}_\infty$ ($X = PF_6^-$, AsF_6^-, SbF_6^-) (nine interpenetrating networks) [20,21], $\{[Ag(3,3'\text{-dicyanodiphenylacetylene})_2]ClO_4\}_\infty$ (eight interpenetrating networks) [24] as well as the intermediate pyridylnitrile example $\{[Ag(4\text{-cyanopyridine})_2]BF_4\}_\infty$ (four interpenetrating networks) [8]. As summarised in Table 1, the number of interpenetrating adamantoid networks can be controlled within any group of complexes; lengthening of the

Table 1
Data on interpenetrating coordination polymers

Complex	No. of interpenetrating adamantoid networks	M···M (Å)	Ref.
$\{[Cu(diaz)_2]PF_6\}_\infty$	3	10.904	[9]
$\{[Cu(4,4'\text{-bipy})_2]BF_4\}_\infty$	4	11.16	[6]
$\{[Ag(4,4'\text{-bipy})_2]CF_3SO_3\}_\infty$	4	11.57–11.61	[8]
$\{[Cu(bpe)_2]PF_6\}_\infty$	5	13.55	[7]
$\{[Ag(4\text{-cyanopyridine})_2]BF_4\}_\infty$	4	9.93	[8]
$\{[Ag(3,3'\text{-dicyanodiphenylacetylene})_2]ClO_4\}_\infty$	8	17.02	[24]
$\{[Ag(4,4'\text{-biphenyldicarbonitrile})_2]X\}_\infty$ ($X = PF_6^-$, AsF_6^-, SbF_6^-)	9	16.42	[20,21]

ligand increases the degree of interpenetration while increased lateral ligand bulk decreases it.

During attempts to characterise further the effect of ligand functionality upon network topology, the coordination chemistry of 1,4-bis(4-pyridyl)-butadiyne (pybut) was investigated. Somewhat surprisingly the reaction between pybut and $[Cu(MeCN)_4]PF_6$ did not produce a diamondoid network but rather a polycatenated molecular ladder [11]. The reaction of $[Cu(MeCN)_4]PF_6$ with 1,4-bis-(4-pyridyl)butadiyne (pybut) in $MeCN/CH_2Cl_2$ yields a deep red solution from which red crystals of composition $\{[Cu_2(MeCN)_2(pybut)_3](PF_6)_2\}_\infty$ were isolated by infusion of Et_2O. Even in the presence of a large excess of ligand (up to a metal:ligand ratio of 1:4) the same product was isolated. X-ray diffraction studies of these crystals show that the compound exists as a molecular ladder in which each Cu(I) centre is coordinated in a tetrahedral geometry to three pybut ligands, Cu–N = 1.993(9)–2.115(10) Å, and one MeCN ligand, Cu–N = 1.978(13), 1.994(12) Å, (Fig. 6). The ladder structure is generated via the pybut ligands which each bridge two Cu(I) centres. This structure is somewhat surprising as insoluble adamantoid networks have been the previously observed, and expected, product from this type of reaction [6–9]. Molecular ladders have been observed for relatively few related systems, and in all previous cases the metal junction of the ladder has been pseudo-octahedral in $[Co_2(4,4'\text{-bipy})_3(NO_3)_4]_\infty$ [12] and $[Cd_2(L)_3](NO_3)_4]_\infty$ (L = 1,4-

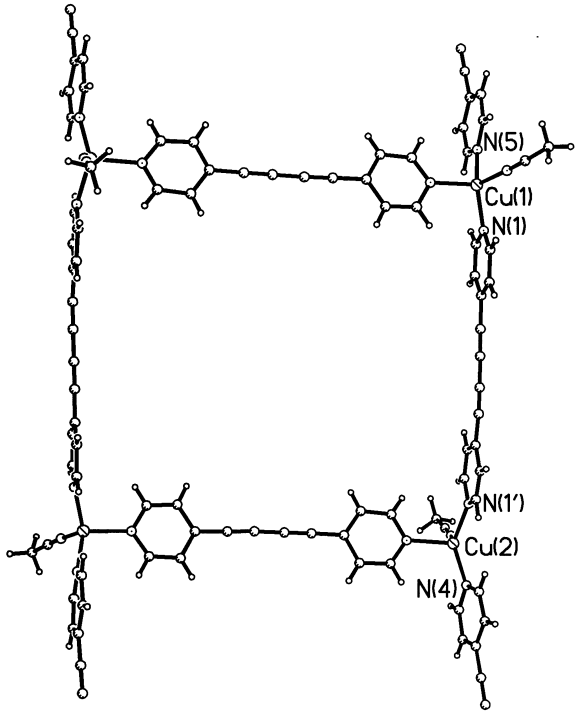

Fig. 6. Part of the molecular ladder formed by $\{[Cu_2(MeCN)_2(pybut)_3](PF_6)_2\}_\infty$ [11].

bis(4-methylpyridyl)benzene) [15]) generating what may be termed a flat ladder with all linking ligands co-planar. In the case reported here the tetrahedral Cu(I) centres allow the ladder to undulate with the large cavities between the rungs of the ladder filled by four independent, symmetry-related ladders. Thus, each ladder is polycatenated by a further four ladders which weave through the first so as to fill the spaces between its rungs (Fig. 7). Polycatenation of symmetry-related ladders occurs also in $[Cd_2(L)_3](NO_3)_4]_\infty$ [15], although the interpenetration is perpendicular to the orientation of the original ladder rather than parallel to it as in $\{[Cu_2(MeCN)_2(pybut)_3](PF_6)_2\}_\infty$. In $[Co_2(4,4'\text{-bipy})_3(NO_3)_4]_\infty$ no catenation is observed [12]. In $\{[Cu_2(MeCN)_2(pybut)_3](PF_6)_2\}_\infty$ the parallel polycatenated ladders form a 2D sheet with distortion of the N(1)–Cu(1)–N(5) and N(1′)–Cu(2)–N(4) angles from tetrahedral to 128.4(4) and 124.9(4)°, respectively, allowing a significant flattening of each ladder (Fig. 8). $\pi-\pi$ interactions with adjacent symmetry-related ladders at distances of 3.484 Å presumably contribute to the stability of the observed structural motif. The 2D sheets of interwoven ladders are separated by PF_6^- counter-anions and solvent molecules with the coordinated MeCN molecules pointing toward the next sheet in the crystal. The structure of $\{[Cu_2(MeCN)_2(pybut)_3](PF_6)_2\}_\infty$ represents a unique polycatenated undulating molecular ladder which forms interwo-

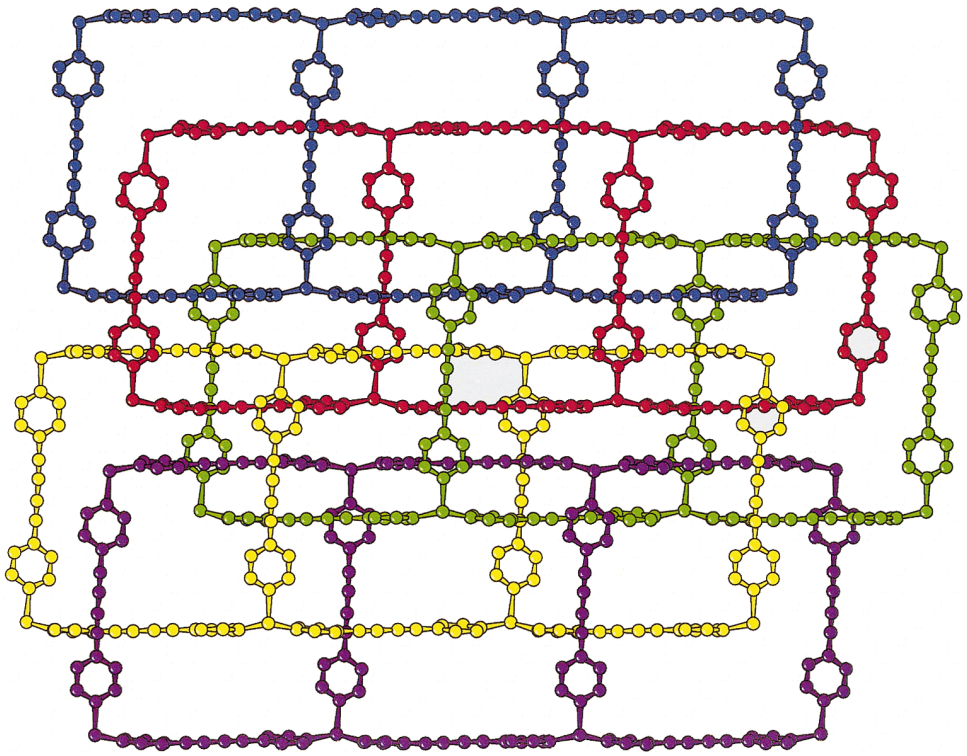

Fig. 7. View of $\{[Cu_2(MeCN)_2(pybut)_3](PF_6)_2\}_\infty$ illustrating how each molecular ladder is polycatenated by four other ladders (reproduced with permission from Ref. [11]).

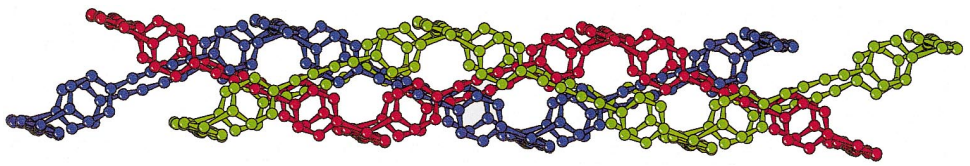

Fig. 8. View of $\{[Cu_2(MeCN)_2(pybut)_3](PF_6)_2\}_\infty$ showing the undulating nature of the ladders which allows them to interweave in a parallel fashion (reproduced with permission from Ref. [11]).

ven 2D sheets, an unprecedented structural motif in inorganic coordination polymers. We are currently investigating the factors that favour the formation of molecular ladders over the more common adamantoid networks seen for Cu(I) bipyridyl systems.

Zig-zag chains are also a feature of the structures of the products isolated from the reaction of $[Cu(MeCN)_4]BF_4$ with one equivalent of bipyridyl ligand (L = 4,4-bipy [25], 3-pytz (1,4-bis-(3-pyridyl)-2,3,4,5-tetrazine) [26], or 4-pytz (1,4-bis-(4-pyridyl)-2,3,4,5-tetrazine) [26]) in MeCN. Fig. 9 shows the structure of $\{[Cu(4,4'\text{-bipy})(MeCN)_2]^+\}_\infty$ as a representative example. In each case each Cu(I) centre is coordinated to two bridging pyridyl ligands and to two MeCN ligands. These chains represent the simplest form of polymer formed by Cu(I)–bipyridyl species and may be regarded as an intermediate which acts as a potential building block for the formation of adamantoid networks and molecular ladders.

3. Chains, ladders and sheets in silver(I)–bipyridyl chemistry

Our studies of the Ag(I) complexes formed with ligands based upon 4,4-bipyridyl reveal a preference for linear chains of alternating Ag(I) ions and bipyridyl ligands

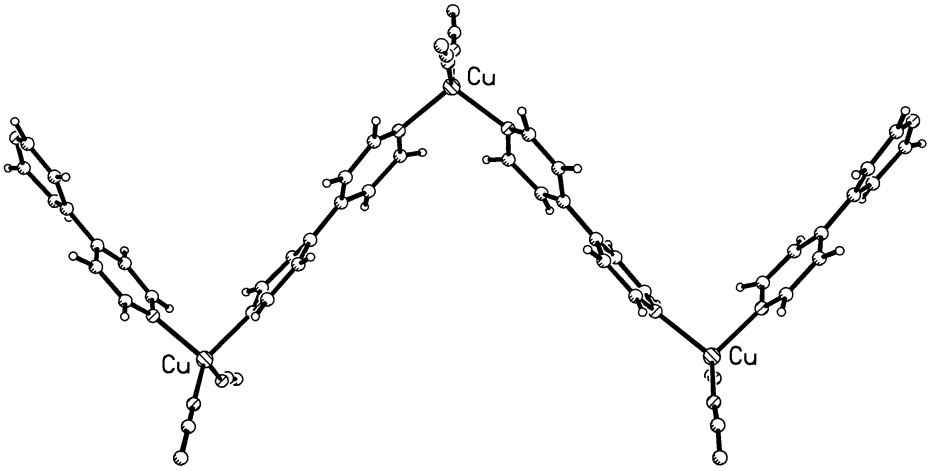

Fig. 9. View of the zig-zag chains formed by $\{[Cu(MeCN)_2(4,4\text{-bipy})]BF_4\}_\infty$.

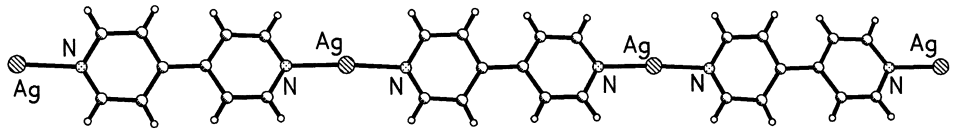

Fig. 10. View of the linear chains formed by $\{[Ag(4,4'\text{-bipy})]BF_4\}_\infty$.

when products are prepared in the presence of weakly coordinating solvents such as MeCN or PhCN. This is unsurprising given the strong preference of Ag(I) for linear geometry [22,27]. However, the packing of these chains in the solid state reveals a remarkable dependence upon both ligand functionality and anion coordinative ability.

3.1. Effect of ligand functionality

In order to assess the effect of ligand functionality on the solid-state packing of chains, Ag–bipyridyl complexes were prepared in the form of salts with weakly coordinating anions, such as BF_4^- or PF_6^- [28].

In $\{[Ag(4,4'\text{-bipy})]BF_4\}_\infty$ alternating Ag(I) ions and 4,4′-bipy ligands form linear chains, (Fig. 10) which lie parallel within the crystal structure but are staggered, thereby minimising Ag···Ag contacts and also minimising $\pi-\pi$ interactions between adjacent chains, (Fig. 11) [29].

In contrast, the structure of $\{[Ag(pybut)](PO_2F_2)\}_\infty$ contains [30] pairs of linear chains of alternating Ag(I) ions and bipyridyl ligands, resembling a ladder structure in which the ligands form $\pi-\pi$ interactions of 3.394 Å and Ag···Ag interactions of 3.1929(10) Å, (Fig. 12) [31]. A similar ladder-like motif in which chains are paired is observed also for the isostructural salts $\{[Ag(4\text{-pytz})]X\}_\infty$ ($X = BF_4^-$, PF_6^- Fig. 13) [14] and for $\{[Ag(3\text{-pytz})]CF_3SO_3\}_\infty$ [26] (Fig. 14) with Ag···Ag interactions of 3.312(1), 3.230(1) and 3.2199(13) Å, respectively [14].

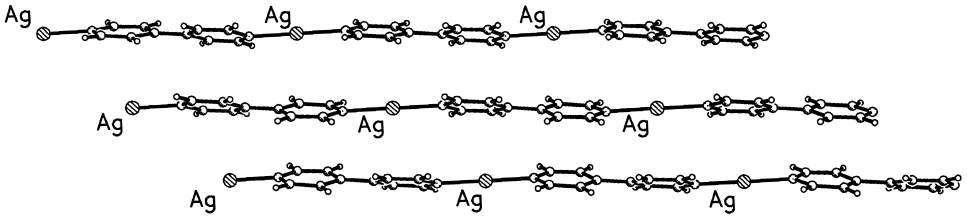

Fig. 11. View of the staggered $\{[Ag(4,4'\text{-bipy})]BF_4\}_\infty$ chains, minimising Ag···Ag contacts and $\pi-\pi$ interactions between adjacent chains.

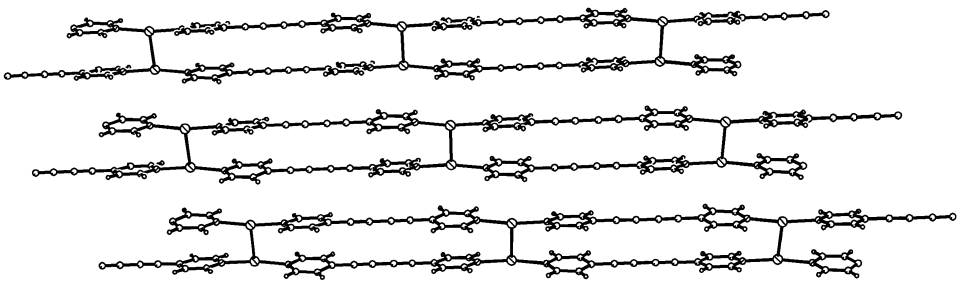

Fig. 12. View of the pairs of linear chains observed in $\{[Ag(pybut)]PO_2F_2\}_\infty$, in which the ligands form $\pi-\pi$ interactions of 3.394 Å and relatively short Ag···Ag interactions of 3.1929(10) Å.

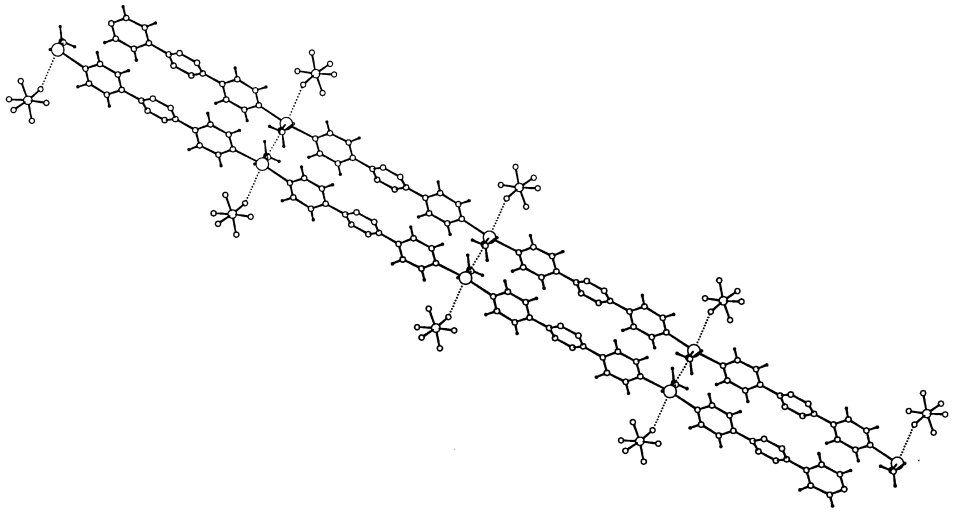

Fig. 13. View of the pairs of linear chains formed by $\{[Ag(4\text{-pytz})]X\}_\infty$ ($X = BF_4^-$, PF_6^-). (Ag···Ag = 3.312(1) Å (BF_4^-), 3.230(1) Å (PF_6^-)] (reproduced with permission from Ref. [14]).

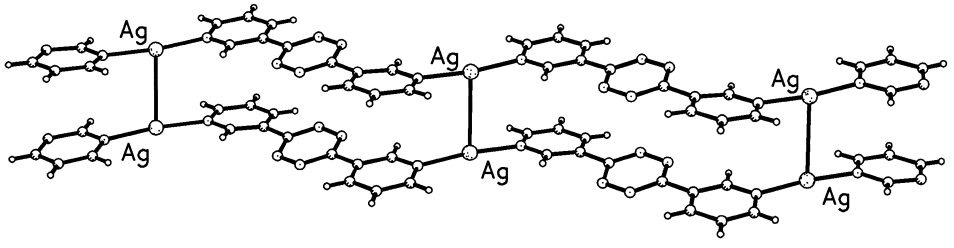

Fig. 14. View of the pairs of linear chains formed by $\{[Ag(3\text{-pytz})]CF_3SO_3\}_\infty$, [Ag···Ag = 3.2199(13) Å].

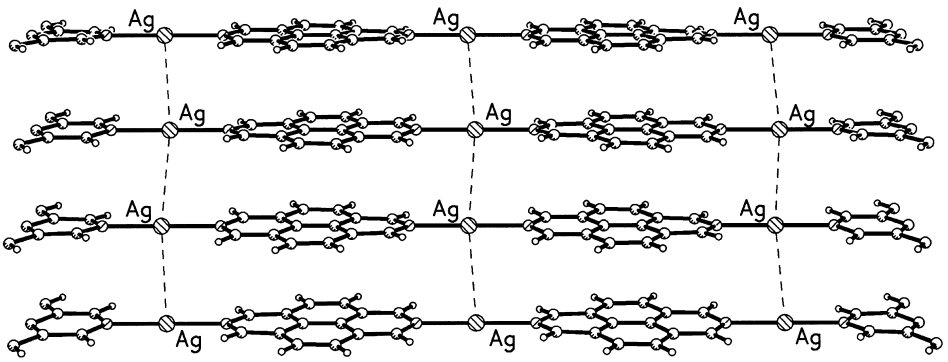

Fig. 15. View of the π–π stacked linear chains observed for $\{[Ag(diaz)]BF_4\}_\infty$ (reproduced with permission from Ref. [9]).

The related Ag(I) complex with 2,7-diazapyrene, $\{[Ag(diaz)]BF_4\}_\infty$, has also been prepared and structural characterisation reveals a similar linear chain motif, (Fig. 15) [9]. Interestingly, these chains are linked together by face-to-face π–π interactions between 2,7-diazapyrene ligands in which the ligand N···N axes lie parallel to each other at a distance of 3.380 Å (cf. 3.450 Å for the free ligand) [23]. In this case the Ag···Ag contact is considerably longer at 3.640 Å. Bonding between adjacent chains is further strengthened by MeCN ligands bridging adjacent Ag centres, Ag–N = 2.871(4)–2.926(4) Å, to form 2D sheets. The increased π–π stacking ability of 2,7-diazapyrene encourages not only the formation of pairs of chains, or ladders, but the formation of a sheet structure with extended π–π stacking interactions.

To summarise, it can be seen that by increasing the ability of the ligand to form π–π interactions we have encouraged the construction of longer-range arrays. This progression can be seen from the simple linear chains of $\{[Ag(4,4'\text{-bipy})]BF_4\}_\infty$ to the ladders of $\{[Ag(pybut)](PO_2F_2)\}_\infty$ [30] and $\{[Ag(4\text{-pytz})]X\}_\infty$ ($X = BF_4^-$, PF_6^-) [14] and to the 2D sheets of $\{[Ag(diaz)]BF_4\}_\infty$.

3.2. Effect of anion functionality

We have also investigated the effect of anion upon the long-range order of Ag(I)–bipyridyl complexes. In particular, replacement of the weakly coordinating BF_4^- and PF_6^- anions by more strongly coordinating NO_3^- anions has a profound effect upon network geometry.

The effect of the change in anion is perhaps most notable in the case of the Ag(I) complexes with 4-pytz [14]. In contrast to the linear chain complexes $\{[Ag(4\text{-pytz})]PF_6\}_\infty$ and $\{[Ag(4\text{-pytz})]BF_4\}_\infty$, the complex formed between $AgNO_3$ and 4-pytz forms what may be termed a helical staircase structure [14]. The structure of the complex comprises Ag(I) ions each coordinated to two 4-pytz ligands in a linear arrangement to give linear chains of alternating Ag(I) ions and bipyridyl ligands. Each Ag(I) ion also exhibits weak interactions with two NO_3^- ions, Ag···O =

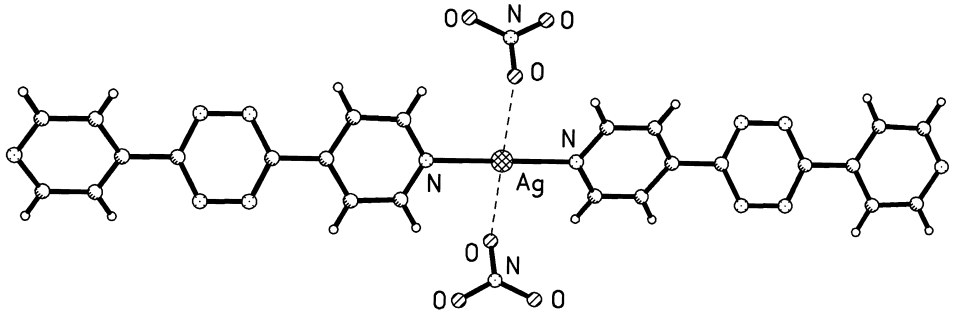

Fig. 16. View of the pseudo-square planar geometry of the Ag(I) ion in $\{[Ag(4\text{-pytz})]NO_3\}_\infty$.

2.787(2) Å, which adopt positions perpendicular to the pyridyl–Ag–pyridyl axis to afford a pseudo-square planar geometry at Ag(I), (Fig. 16). These NO_3^- ions bridge adjacent Ag–bipyridyl chains through two of their oxygen atoms so that each Ag(I) chain is related to the next by a 60° rotation and a step of 5.18 Å, generating a helical staircase (Fig. 17). Thus, it can be seen that the 3D structure is controlled via the

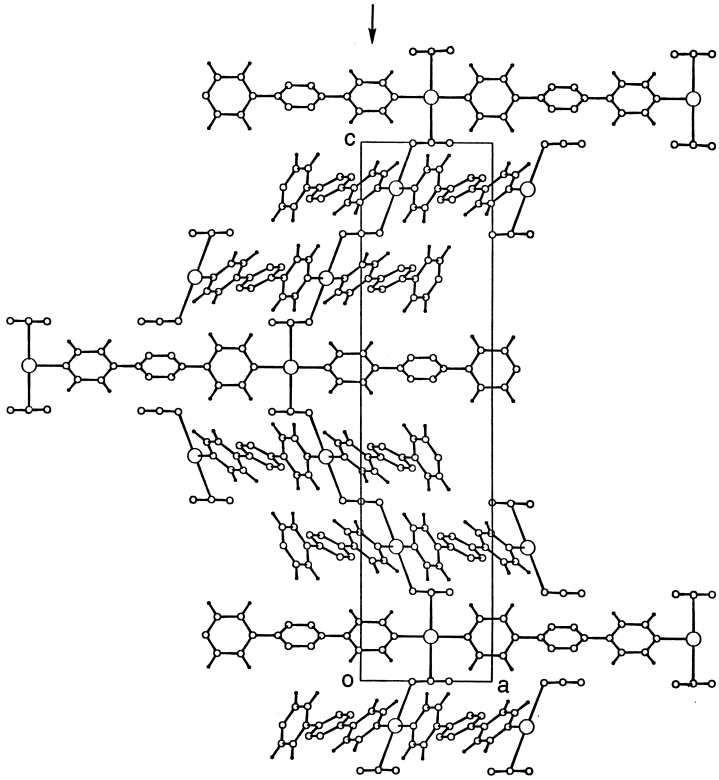

Fig. 17. View of the helical staircase motif formed by $\{[Ag(4\text{-pytz})]NO_3\}_\infty$ (reproduced with permission from Ref. [14]).

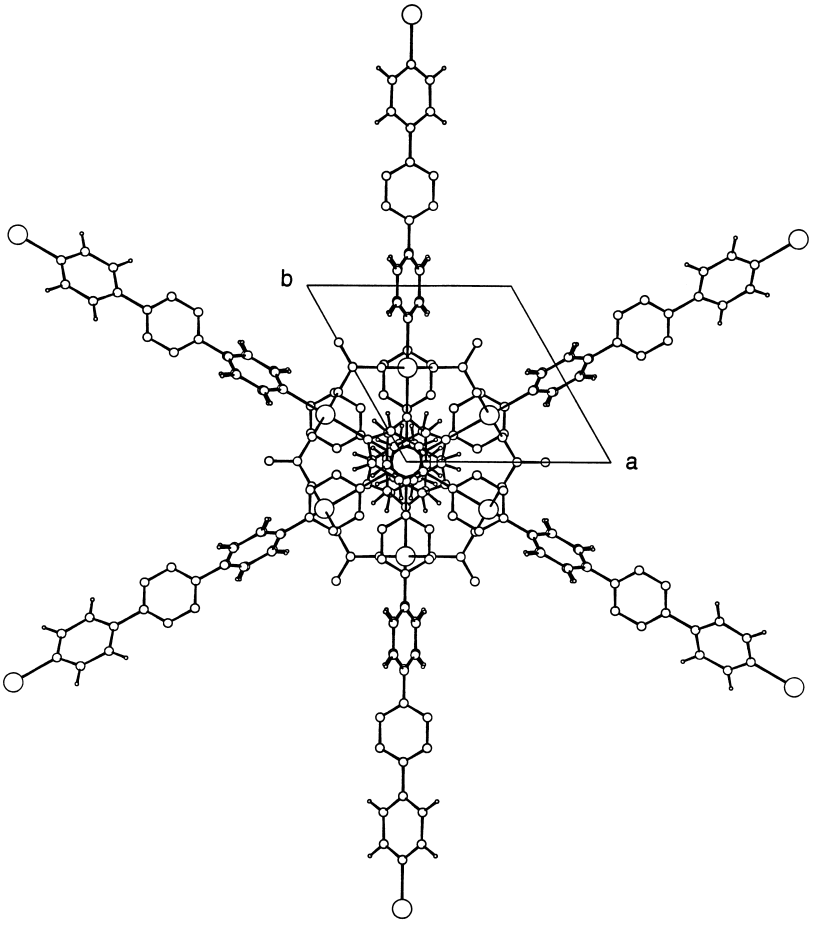

Fig. 18. View of $\{[Ag(4\text{-pytz})]NO_3\}_\infty$ along the helical axis illustrating the hexagonal arrangement of the polymeric chains (reproduced with permission from Ref. [14]).

$Ag–ONO_2$ interactions. The points at which the chains cross, which one may consider the centre of the helix, correspond to pyridyl units of the overlapping ligand, (Fig. 18). Very recently, Robson and co-workers have reported [32] a related helical structure, also in space group $P6_122$, for the coordination polymer $Cd(tcm)[B(OMe)_4]$ (tcm = tricyanomethanide, $C(CN)_3^-$].

The effect of anion functionality is also illustrated by the complexes formed by Ag(I) with pybut. As already discussed, the complex $\{[Ag(pybut)](PO_2F_2)\}_\infty$ [30] forms linear chains of alternating Ag(I) ions and bipyridyl ligands in which pairs of chains are linked via $\pi–\pi$ interactions and Ag···Ag interactions to give a ladder structure, (see Section 3.1 and Fig. 12). Introduction of NO_3^- anions also leads to the formation of linear chains consisting of alternating Ag(I) ions and pybut ligands [30]. However, in the case of $[\{Ag(pybut)]NO_3\}_\infty$ these chains no longer link pairwise to form ladders with Ag···Ag interactions. Instead the Ag···Ag and $\pi–\pi$

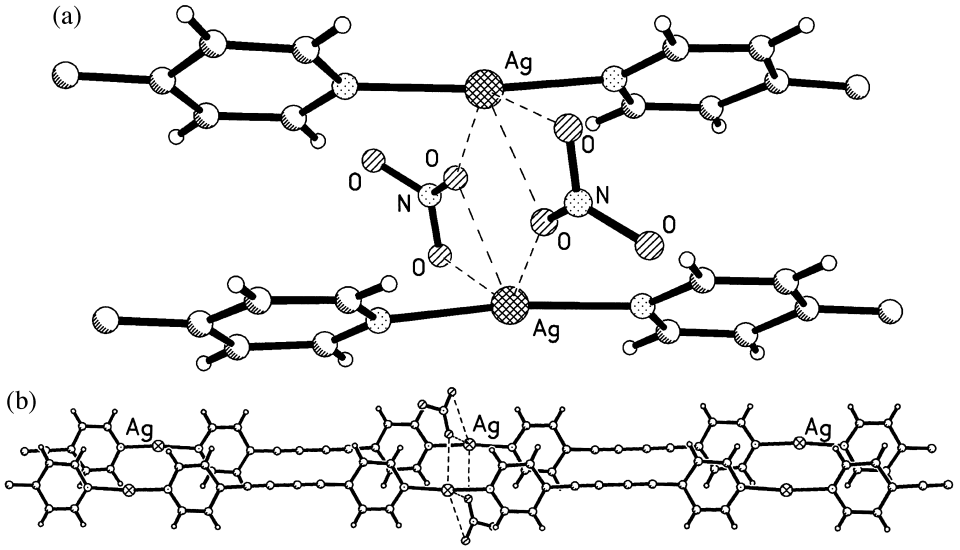

Fig. 19. (a) View illustrating the role of the weak interactions between Ag(I) ions and NO_3^- anions in $[\{Ag(pybut)]NO_3\}_\infty$ leading to (b) staggered pairs of chains of $[\{Ag(pybut)]NO_3\}_\infty$.

interactions are replaced with weak interactions to the NO_3^- anion. These weakly coordinating NO_3^- anions bridge between adjacent chains so as to form staggered pairs of chains, (Fig. 19).

In the case of the Ag(I) complexes of 2,7-diazapyrene the effect of $\pi-\pi$ interactions is much stronger, hence the complex $\{[Ag(diaz)]NO_3\}_\infty$ exhibits a structure similar to that observed for $\{[Ag(diaz)]BF_4\}_\infty$. Each Ag(I) centre is coordinated by two diaz ligands and by a bidentate nitrate anion. This imparts a twist to the resultant chain with an angle of 144.2(2)° (N–Ag–N) between the diaz ligands at each Ag(I) centre, (Fig. 20) [30]. These undulating chains then stack via $\pi-\pi$ interactions, 3.339 Å (vs. 3.450 Å for the free ligand and 3.380 Å

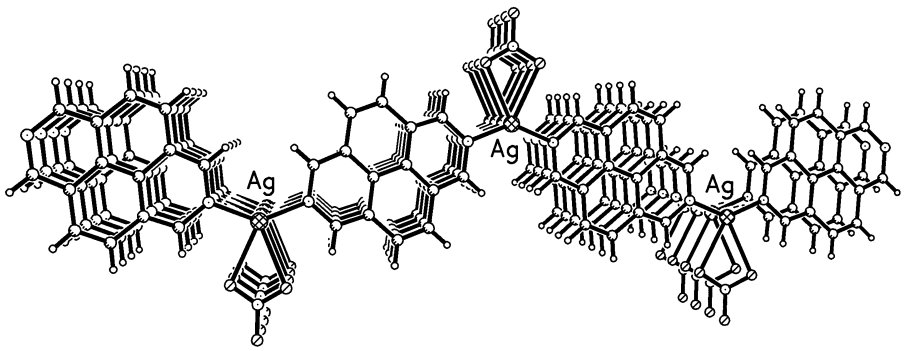

Fig. 20. View of the undulating chains of $\{[Ag(diaz)]NO_3\}_\infty$ which stack to give a two-dimensional sheet through $\pi-\pi$ interactions (3.339 Å).

for $\{[Ag(diaz)]BF_4\}_\infty$), to give a 2D sheet which is similar to that observed for the corresponding BF_4^- salt. The remarkable similarity between the structures of $\{[Ag(diaz)]NO_3\}_\infty$ and $\{[Ag(diaz)]BF_4\}_\infty$ shows that $\pi-\pi$ interactions have a strong influence over the structure of 2,7-diazapyrene complexes.

The structure of $\{[Ag(4,4'\text{-bipy})]NO_3\}_\infty$ reveals a different structural motif with orthogonal linear chains linked via Ag···Ag contacts of 2.970(2) Å, (Fig. 21) [33]. This contrasts with both the structure of $\{[Ag(4,4'\text{-bipy})]BF_4\}_\infty$ [29] (Figs. 10 and 11) and with the other structural motifs that we have observed with other Ag–bipyridyl nitrate complexes (Figs. 19 and 20). The range of different structural motifs observed with these Ag–bipyridyl complexes emphasises the subtle effects that ligand functionality and anion structure can exert upon long-range order in these structures.

Comparison with related dinitrile systems is less appropriate in the case of Ag(I) polymers than in the Cu(I) and adamantoid cases described in Section 2, as Ag(I) polymers are markedly more sensitive to ligand and anion functionality and to solvent systems. Thus, within a related series of complexes, all grown under similar conditions, comparison can lead to a greater understanding of the individual contributions of ligand and anion functionality.

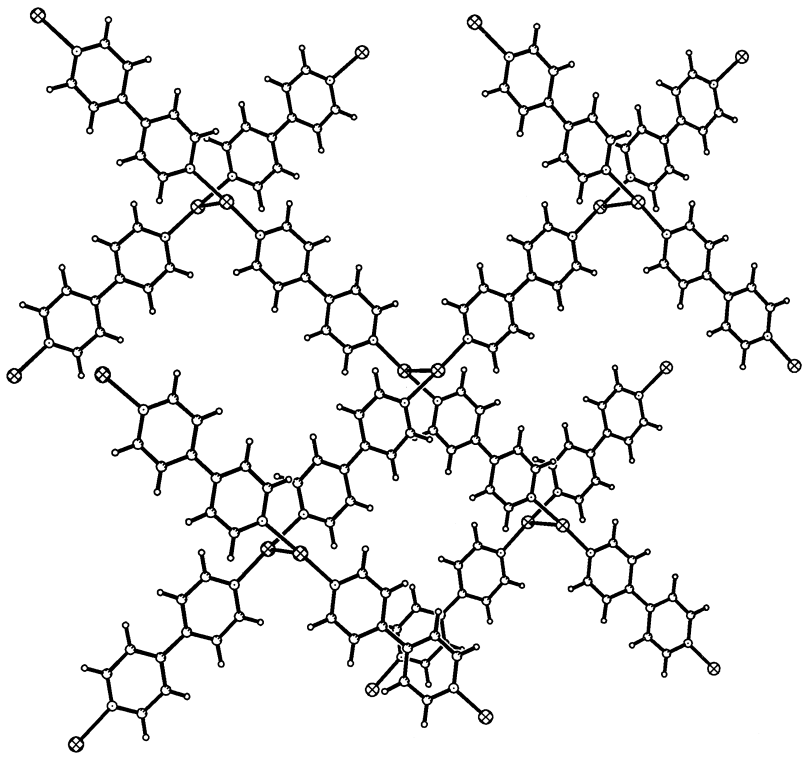

Fig. 21. View of the structure of $\{[Ag(4,4'\text{-bipy})]NO_3\}_\infty$ showing the orthogonal linear chains linked via Ag···Ag contacts [33].

However, comparisons between related systems are less valid when different ligating groups or solvent systems are employed. Moore et al. have reported [20–22,24] some elegant studies on the chemistry of Ag(I) complexes with a wide range of dinitrile ligands, leading to a range of unusual arrays and network topologies.

3.3. In situ ligand synthesis and lattice construction

The reaction of $AgBF_4$ and bpe [bpe = 1,2-*trans*-bis(4-pyridyl)ethene] does not yield a linear chain complex: in this case the ligand dimerises to form a cyclobutane ring substituted by four 4-pyridyl rings [34]. This ligand is bound to a Ag(I) ion through all four of its pyridyl rings (Fig. 22) with each Ag(I) ion bound to four 1,2,3,4-*tetrakis*(4-pyridyl)cyclobutane [(4-py)cyb] ligands to form a 3D array, (Fig. 23). The structure incorporates counter-anions, in this case BF_4^-, which are accommodated in channels running through the array. These channels are intriguing in that the Ag–pyridyl–cyclobutane–pyridyl–Ag chain forms a helix which winds around the channel. The handedness of this helix alternates along adjacent channels thus giving the structure no overall chirality. The network topology represented by this structure is unprecedented.

Photolytic dimerisation of 1,2-*trans*-bis(4-pyridyl)ethene in solution requires UV radiation and yields two isomers of the ligand (4-py)-cyb [35], in contrast to the single isomer observed in our product (as evidenced by ^{1}H-NMR spectroscopy of the bulk product). Thus, we believe that the formation of linear

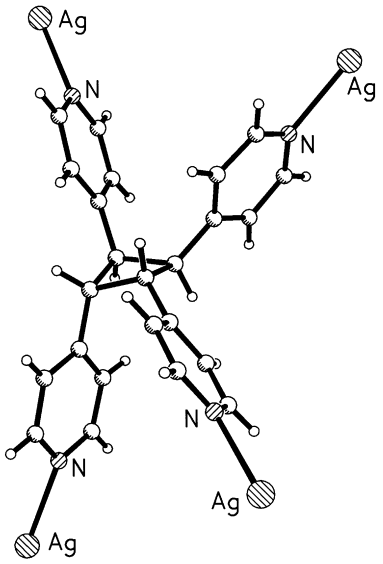

Fig. 22. View of the ligand 1,2,3,4-tetrakis(4-pyridyl)cyclobutane {(4-py)cyb}, formed by the dimerisation of bpe, linked to four Ag(I) ions [34].

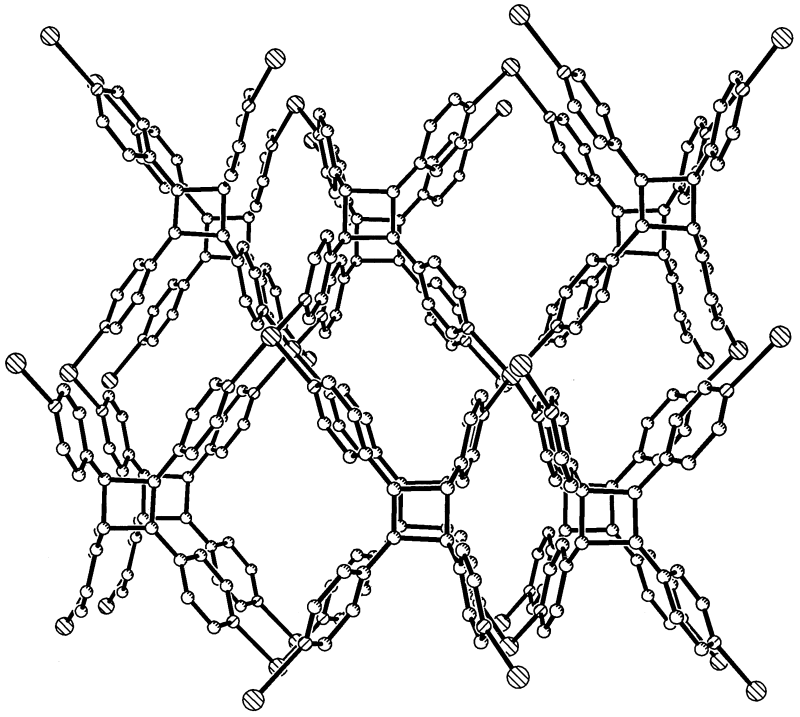

Fig. 23. View of the three-dimensional array formed by $\{[Ag\{(4\text{-py})cyb\}]BF_4\}_\infty$ (reproduced with permission from Ref. [34]).

chains of Ag–bpe units (already shown to be a common structural motif for silver–bipyridyl complexes) places the ethene linkages in close proximity, (Fig. 24) which is presumably a necessary pre-condition of the dimerisation. This close proximity of the double bonds lowers the activation barrier to dimerisation, as first shown by Schmidt [36], while coordination to Ag(I) shifts the electronic transition further into the visible region. This is consistent with the formation of only one observed isomer of the ligand.

These results illustrate that the long-range order of the bipyridyl complexes, in this case their tendency to form pairs of linear chains linked by Ag···Ag contacts, can be used to facilitate interesting chemistry leading to the formation of

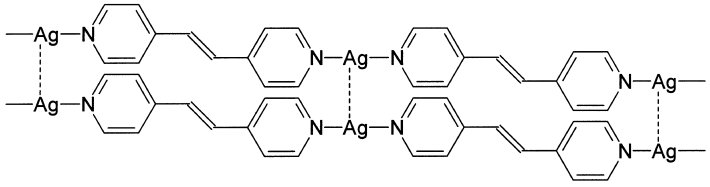

Fig. 24. Pairs-of-chains motif expected for $\{[Ag(bpe)]BF_4\}_\infty$, which places the ethene linkages in close proximity (reproduced with permission from Ref. [34]).

unprecedented network topologies. This in situ ligand synthesis and lattice construction represents a potential new direction for inorganic crystal engineering.

4. Conclusions and future developments

In this article we have reported a range of unusual structures including adamantoid arrays, polycatenated molecular ladders and a helical staircase. These unusual structures demonstrate that the functionality of the building block used in network construction can be used to control overall structure of the array. Whether transition metal, ligand or anion, the functionality of these building blocks has a gross effect upon the nature of the network observed. It has also been illustrated that network structure can be used to promote chemical reactions and to control ligand synthesis. We are currently developing the chemistry reported here in the pursuit of materials with interesting intercalative or electronic properties.

Acknowledgements

The authors would like to thank the EPSRC, Nuffield Foundation and the University of Nottingham for support.

References

[1] G.R. Desiraju, in: Crystal Engineering: Design of Organic Solids, Elsevier, Amsterdam, 1989.
[2] G.R. Desiraju (Ed.), The Crystal as a Supramolecular Entity, Wiley, New York, 1995.
[3] G.R. Desiraju, Angew. Chem. 107 (1995) 2541; Angew. Chem. Int. Ed. Engl. 34 (1995) 2311.
[4] R. Robson, B.F. Abrahams, S.R. Batten, R.W. Gable, B.F. Hoskins, J. Liu, Supramolecular Architecture, ACS, Washington, DC, 1992, Ch. 19.
[5] M. Fujita, Y.J. Kwon, S. Washizu, K. Ogura, J. Am. Chem. Soc. 116 (1994) 1151.
[6] L.R. MacGillvary, S. Subramanian, M.J. Zaworotko, J. Chem. Soc. Chem. Commun. (1994) 1325.
[7] A.J. Blake, N.R. Champness, S.S.M. Chung, W.-S. Li, M. Schröder, Chem. Commun. (1997) 1005.
[8] L. Carlucci, G. Ciani, D.M. Proserpio, A. Sironi, J. Chem. Soc. Chem. Commun. (1994) 2755.
[9] A.J. Blake, N.R. Champness, A.N. Khlobystov, D.A. Lemenovski, W.-S. Li, M. Schröder, Chem. Commun. (1997) 1339.
[10] S. Subramanian and M.J. Zaworotko, Angew. Chem. 107 (1995) 2295; Angew. Chem. Int. Ed. Engl. 34 (1995) 2127.
[11] A.J. Blake, N.R. Champness, A.N. Khlobystov, D.A. Lemenovskii, W.-S. Li, M. Schröder, Chem. Commun. (1997) 2027.
[12] P. Losier and M.J. Zaworotko, Angew. Chem. 108 (1996) 2957; Angew. Chem. Int. Ed. Engl. 35 (1996) 2779.
[13] G.B. Gardner, D. Venkataraman, J.S. Moore, S. Lee, Nature 374 (1995) 792.
[14] M.A. Withersby, A.J. Blake, N.R. Champness, P. Hubberstey, W.-S. Li, M. Schröder, Angew. Chem. 109 (1997) 2421; Angew. Chem. Int. Ed. Engl. 36 (1997) 2327.
[15] M. Fujita, Y.J. Kwon, O. Sasaki, K. Yamaguchi, K. Ogura, J. Am. Chem. Soc. 117 (1995) 7287.
[16] O. Ermer, Adv. Mater. 3 (1991) 608.
[17] For examples see: (a) O. Ermer, J. Am. Chem. Soc. 110 (1988) 3747. (b) O. Ermer, L. Lindenberg,

Helv. Chim. Acta 74 (1991) 825. (c) O. Ermer, L. Lindenberg, Chem. Ber. 123 (1990) 1111. (d) O. Ermer, L. Lindenberg, Helv. Chim. Acta 71 (1988) 1084.
[18] (a) S.B. Copp, S. Subramanian, M.J. Zaworotko, J. Am. Chem. Soc. 114 (1992) 8719. (b) S.B. Copp, S. Subramanian, M.J. Zaworotko, J. Chem. Soc. Chem. Commun. (1993) 1078. (c) S.B. Copp, K.T. Holman, J.O.S. Sangster, S. Subramanian, M.J. Zaworotko, J. Chem. Soc. Dalton Trans. (1995) 2233. (d) M.J. Zaworotko, Chem. Soc. Rev. (1994) 283.
[19] (a) B.F. Hoskins, R. Robson, J. Am. Chem. Soc. 111 (1989) 5962. (b) B.F. Hoskins, R. Robson, J. Am. Chem. Soc. 112 (1990) 1546.
[20] K.A. Hirsch, D. Venkataraman, S.R. Wilson, J.S. Moore, S. Lee, J. Chem. Soc. Chem. Commun. (1995) 2199.
[21] K.A. Hirsch, S.R. Wilson, J.S. Moore, Chem. Eur. J. 3 (1997) 765.
[22] D. Venkataraman, S. Lee, J.S. Moore, P. Zhang, K.A. Hirsch, G.B. Gardner, A.C. Covey, C.L. Prentice, Chem. Mater. 8 (1996) 2030.
[23] A.J. Blake, N.R. Champness, A.N. Khlobystov, W.-S. Li, M. Schröder, unpublished results.
[24] K.A. Hirsch, S.R. Wilson, J.S. Moore, Inorg. Chem. 36 (1997) 2960.
[25] A.S. Batsanov, M.J. Begley, P. Hubberstey, J. Stroud, J. Chem. Soc. Dalton Trans. (1996) 1947.
[26] M.A. Withersby, A.J. Blake, N.R. Champness, P. Hubberstey, W.-S. Li, M. Schröder, unpublished results.
[27] D. Venkataraman, Y. Du, S.R. Wilson, K.A. Hirsch, P. Zhang, J.S. Moore, J. Chem. Educ. 74 (1997) 915.
[28] W. Beck, K. Sunkel, Chem. Rev. 88 (1988) 1405.
[29] A.J. Blake, N.R. Champness, S.S.M. Chung, W.-S. Li, M. Schröder, unpublished results.
[30] A.J. Blake, N.R. Champness, A.N. Khlobystov, D.A. Lemenovski, W.-S. Li, M. Schröder, unpublished results.
[31] (a) P. Pyykko, Chem. Rev. 97 (1997) 597. (b) G.W. Eastland, M.A. Mazid, D.R. Russell, M.C.R. Symons, J. Chem. Soc. Dalton Trans. (1980) 1682.
[32] S.R. Batten, B.F. Hoskins, R. Robson, Angew. Chem. 109 (1997) 652; Angew. Chem. Int. Ed. Engl. 36 (1997) 636.
[33] (a) F. Robinson, M. Zaworotko, J. Chem. Soc. Chem. Commun. (1995) 2413. (b) O.M. Yaghi, H. Li, J. Am. Chem. Soc. 118 (1996) 295.
[34] A.J. Blake, N.R. Champness, S.S.M. Chung, W.-S. Li, M. Schröder, Chem. Commun. (1997) 1675.
[35] (a) J. Vansant, S. Toppet, G. Smets, J.P. Declerq, G. Germain, M. van Meerssche, J. Org. Chem. 45 (1980) 1565. (b) M. Horner, S. Hunig, Liebigs Ann. Chem. (1982) 1183.
[36] (a) M.D. Cohen, G.M.J. Schmidt, J. Chem. Soc. (1964) 1996. (b) M.D. Cohen, G.M.J. Schmidt, F. Sonntag, J. Chem. Soc. (1964) 2000. (c) G.M.J. Schmidt, J. Chem. Soc. (1964) 2014.